First Measurement of the Ratio of Central-Electron to Forward-Electron W Partial Cross Sections in $p\bar{p}$ Collisions at $\sqrt{s} = 1.96$ TeV.

A. Abulencia,[24] J. Adelman,[13] T. Affolder,[10] T. Akimoto,[56] M.G. Albrow,[17] D. Ambrose,[17] S. Amerio,[44] D. Amidei,[35] A. Anastassov,[53] K. Anikeev,[17] A. Annovi,[19] J. Antos,[14] M. Aoki,[56] G. Apollinari,[17] J.-F. Arguin,[34] T. Arisawa,[58] A. Artikov,[15] W. Ashmanskas,[17] A. Attal,[8] F. Azfar,[43] P. Azzi-Bacchetta,[44] P. Azzurri,[47] N. Bacchetta,[44] W. Badgett,[17] A. Barbaro-Galtieri,[29] V.E. Barnes,[49] B.A. Barnett,[25] S. Baroiant,[7] V. Bartsch,[31] G. Bauer,[33] F. Bedeschi,[47] S. Behari,[25] S. Belforte,[55] G. Bellettini,[47] J. Bellinger,[60] A. Belloni,[33] D. Benjamin,[16] A. Beretvas,[17] J. Beringer,[29] T. Berry,[30] A. Bhatti,[51] M. Binkley,[17] D. Bisello,[44] R.E. Blair,[2] C. Blocker,[6] B. Blumenfeld,[25] A. Bocci,[16] A. Bodek,[50] V. Boisvert,[50] G. Bolla,[49] A. Bolshov,[33] D. Bortoletto,[49] J. Boudreau,[48] A. Boveia,[10] B. Brau,[10] L. Brigliadori,[5] C. Bromberg,[36] E. Brubaker,[13] J. Budagov,[15] H.S. Budd,[50] S. Budd,[24] K. Burkett,[17] G. Busetto,[44] P. Bussey,[21] K. L. Byrum,[2] S. Cabrera^{o},[16] M. Campanelli,[20] M. Campbell,[35] F. Canelli,[17] A. Canepa,[49] S. Carillo^{i},[18] D. Carlsmith,[60] R. Carosi,[47] S. Carron,[34] M. Casarsa,[55] A. Castro,[5] P. Catastini,[47] D. Cauz,[55] M. Cavalli-Sforza,[3] A. Cerri,[29] L. Cerrito^{m},[43] S.H. Chang,[28] Y.C. Chen,[1] M. Chertok,[7] G. Chiarelli,[47] G. Chlachidze,[15] F. Chlebana,[17] I. Cho,[28] K. Cho,[28] D. Chokheli,[15] J.P. Chou,[22] G. Choudalakis,[33] S.H. Chuang,[60] K. Chung,[12] W.H. Chung,[60] Y.S. Chung,[50] M. Ciljak,[47] C.I. Ciobanu,[24] M.A. Ciocci,[47] A. Clark,[20] D. Clark,[6] M. Coca,[16] G. Compostella,[44] M.E. Convery,[51] J. Conway,[7] B. Cooper,[36] K. Copic,[35] M. Cordelli,[19] G. Cortiana,[44] F. Crescioli,[47] C. Cuenca Almenar^{o},[7] J. Cuevas^{l},[11] R. Culbertson,[17] J.C. Cully,[35] D. Cyr,[60] S. DaRonco,[44] M. Datta,[17] S. D'Auria,[21] T. Davies,[21] M. D'Onofrio,[3] D. Dagenhart,[6] P. de Barbaro,[50] S. De Cecco,[52] A. Deisher,[29] G. De Lentdecker^{c},[50] M. Dell'Orso,[47] F. Delli Paoli,[44] L. Demortier,[51] J. Deng,[16] M. Deninno,[5] D. De Pedis,[52] P.F. Derwent,[17] G.P. Di Giovanni,[45] C. Dionisi,[52] B. Di Ruzza,[55] J.R. Dittmann,[4] P. DiTuro,[53] C. Dörr,[26] S. Donati,[47] M. Donega,[20] P. Dong,[8] J. Donini,[44] T. Dorigo,[44] S. Dube,[53] J. Efron,[40] R. Erbacher,[7] D. Errede,[24] S. Errede,[24] R. Eusebi,[17] H.C. Fang,[29] S. Farrington,[30] I. Fedorko,[47] W.T. Fedorko,[13] R.G. Feild,[61] M. Feindt,[26] J.P. Fernandez,[32] R. Field,[18] G. Flanagan,[49] A. Foland,[22] S. Forrester,[7] G.W. Foster,[17] M. Franklin,[22] J.C. Freeman,[29] I. Furic,[13] M. Gallinaro,[51] J. Galyardt,[12] J.E. Garcia,[47] F. Garberson,[10] A.F. Garfinkel,[49] C. Gay,[61] H. Gerberich,[24] D. Gerdes,[35] S. Giagu,[52] P. Giannetti,[47] A. Gibson,[29] K. Gibson,[48] J.L. Gimmell,[50] C. Ginsburg,[17] N. Giokaris^{a},[15] M. Giordani,[55] P. Giromini,[19] M. Giunta,[47] G. Giurgiu,[12] V. Glagolev,[15] D. Glenzinski,[17] M. Gold,[38] N. Goldschmidt,[18] J. Goldstein^{b},[43] A. Golossanov,[17] G. Gomez,[11] G. Gomez-Ceballos,[11] M. Goncharov,[54] O. González,[32] I. Gorelov,[38] A.T. Goshaw,[16] K. Goulianos,[51] A. Gresele,[44] M. Griffiths,[30] S. Grinstein,[22] C. Grosso-Pilcher,[13] R.C. Group,[18] U. Grundler,[24] J. Guimaraes da Costa,[22] Z. Gunay-Unalan,[36] C. Haber,[29] K. Hahn,[33] S.R. Hahn,[17] E. Halkiadakis,[53] A. Hamilton,[34] B.-Y. Han,[50] J.Y. Han,[50] R. Handler,[60] F. Happacher,[19] K. Hara,[56] M. Hare,[57] S. Harper,[43] R.F. Harr,[59] R.M. Harris,[17] M. Hartz,[48] K. Hatakeyama,[51] J. Hauser,[8] A. Heijboer,[46] B. Heinemann,[30] J. Heinrich,[46] C. Henderson,[33] M. Herndon,[60] J. Heuser,[26] D. Hidas,[16] C.S. Hill^{b},[10] D. Hirschbuehl,[26] A. Hocker,[17] A. Holloway,[22] S. Hou,[1] M. Houlden,[30] S.-C. Hsu,[9] B.T. Huffman,[43] R.E. Hughes,[40] U. Husemann,[61] J. Huston,[36] J. Incandela,[10] G. Introzzi,[47] M. Iori,[52] Y. Ishizawa,[56] A. Ivanov,[7] B. Iyutin,[33] E. James,[17] D. Jang,[53] B. Jayatilaka,[35] D. Jeans,[52] H. Jensen,[17] E.J. Jeon,[28] S. Jindariani,[18] M. Jones,[49] K.K. Joo,[28] S.Y. Jun,[12] J.E. Jung,[28] T.R. Junk,[24] T. Kamon,[54] P.E. Karchin,[59] Y. Kato,[42] Y. Kemp,[26] R. Kephart,[17] U. Kerzel,[26] V. Khotilovich,[54] B. Kilminster,[40] D.H. Kim,[28] H.S. Kim,[28] J.E. Kim,[28] M.J. Kim,[12] S.B. Kim,[28] S.H. Kim,[56] Y.K. Kim,[13] N. Kimura,[56] L. Kirsch,[6] S. Klimenko,[18] M. Klute,[33] B. Knuteson,[33] B.R. Ko,[16] K. Kondo,[58] D.J. Kong,[28] J. Konigsberg,[18] A. Korytov,[18] A.V. Kotwal,[16] A. Kovalev,[46] A.C. Kraan,[46] J. Kraus,[24] I. Kravchenko,[33] M. Kreps,[26] J. Kroll,[46] N. Krumnack,[4] M. Kruse,[16] V. Krutelyov,[10] T. Kubo,[56] S. E. Kuhlmann,[2] T. Kuhr,[26] Y. Kusakabe,[58] S. Kwang,[13] A.T. Laasanen,[49] S. Lai,[34] S. Lami,[47] S. Lammel,[17] M. Lancaster,[31] R.L. Lander,[7] K. Lannon,[40] A. Lath,[53] G. Latino,[47] I. Lazzizzera,[44] T. LeCompte,[2] J. Lee,[50] J. Lee,[28] Y.J. Lee,[28] S.W. Lee^{n},[54] R. Lefèvre,[3] N. Leonardo,[33] S. Leone,[47] S. Levy,[13] J.D. Lewis,[17] C. Lin,[61] C.S. Lin,[17] M. Lindgren,[17] E. Lipeles,[9] A. Lister,[7] D.O. Litvintsev,[17] T. Liu,[17] N.S. Lockyer,[46] A. Loginov,[61] M. Loreti,[44] P. Loverre,[52] R.-S. Lu,[1] D. Lucchesi,[44] P. Lujan,[29] P. Lukens,[17] G. Lungu,[18] L. Lyons,[43] J. Lys,[29] R. Lysak,[14] E. Lytken,[49] P. Mack,[26] D. MacQueen,[34] R. Madrak,[17] K. Maeshima,[17] K. Makhoul,[33] T. Maki,[23] P. Maksimovic,[25] S. Malde,[43] G. Manca,[30] F. Margaroli,[5] R. Marginean,[17] C. Marino,[26] C.P. Marino,[24] A. Martin,[61] M. Martin,[25] V. Martin^{g},[21] M. Martínez,[3] T. Maruyama,[56] P. Mastrandrea,[52] T. Masubuchi,[56] H. Matsunaga,[56] M.E. Mattson,[59] R. Mazini,[34] P. Mazzanti,[5] K.S. McFarland,[50] P. McIntyre,[54] R. McNulty^{f},[30] A. Mehta,[30] P. Mehtala,[23] S. Menzemer^{h},[11] A. Menzione,[47] P. Merkel,[49] C. Mesropian,[51] A. Messina,[36] T. Miao,[17] N. Miladinovic,[6] J. Miles,[33] R. Miller,[36] C. Mills,[10] M. Milnik,[26] A. Mitra,[1] G. Mitselmakher,[18] A. Miyamoto,[27] S. Moed,[20] N. Moggi,[5] B. Mohr,[8] R. Moore,[17]

M. Morello,[47] P. Movilla Fernandez,[29] J. Mülmenstädt,[29] A. Mukherjee,[17] Th. Muller,[26] R. Mumford,[25] P. Murat,[17] J. Nachtman,[17] A. Nagano,[56] J. Naganoma,[58] I. Nakano,[41] A. Napier,[57] V. Necula,[18] C. Neu,[46] M.S. Neubauer,[9] J. Nielsen,[29] T. Nigmanov,[48] L. Nodulman,[2] O. Norniella,[3] E. Nurse,[31] S.H. Oh,[16] Y.D. Oh,[28] I. Oksuzian,[18] T. Okusawa,[42] R. Oldeman,[30] R. Orava,[23] K. Osterberg,[23] C. Pagliarone,[47] E. Palencia,[11] V. Papadimitriou,[17] A.A. Paramonov,[13] B. Parks,[40] S. Pashapour,[34] J. Patrick,[17] G. Pauletta,[55] M. Paulini,[12] C. Paus,[33] D.E. Pellett,[7] A. Penzo,[55] T.J. Phillips,[16] G. Piacentino,[47] J. Piedra,[45] L. Pinera,[18] K. Pitts,[24] C. Plager,[8] L. Pondrom,[60] X. Portell,[3] O. Poukhov,[15] N. Pounder,[43] F. Prakoshyn,[15] A. Pronko,[17] J. Proudfoot,[2] F. Ptohos[e],[19] G. Punzi,[47] J. Pursley,[25] J. Rademacker[b],[43] A. Rahaman,[48] N. Ranjan,[49] S. Rappoccio,[22] B. Reisert,[17] V. Rekovic,[38] P. Renton,[43] M. Rescigno,[52] S. Richter,[26] F. Rimondi,[5] L. Ristori,[47] A. Robson,[21] T. Rodrigo,[11] E. Rogers,[24] S. Rolli,[57] R. Roser,[17] M. Rossi,[55] R. Rossin,[18] A. Ruiz,[11] J. Russ,[12] V. Rusu,[13] H. Saarikko,[23] S. Sabik,[34] A. Safonov,[54] W.K. Sakumoto,[50] G. Salamanna,[52] O. Saltó,[3] D. Saltzberg,[8] C. Sánchez,[3] L. Santi,[55] S. Sarkar,[52] L. Sartori,[47] K. Sato,[17] P. Savard,[34] A. Savoy-Navarro,[45] T. Scheidle,[26] P. Schlabach,[17] E.E. Schmidt,[17] M.P. Schmidt,[61] M. Schmitt,[39] T. Schwarz,[7] L. Scodellaro,[11] A.L. Scott,[10] A. Scribano,[47] F. Scuri,[47] A. Sedov,[49] S. Seidel,[38] Y. Seiya,[42] A. Semenov,[15] L. Sexton-Kennedy,[17] A. Sfyrla,[20] M.D. Shapiro,[29] T. Shears,[30] P.F. Shepard,[48] D. Sherman,[22] M. Shimojima[k],[56] M. Shochet,[13] Y. Shon,[60] I. Shreyber,[37] A. Sidoti,[47] P. Sinervo,[34] A. Sisakyan,[15] J. Sjolin,[43] A.J. Slaughter,[17] J. Slaunwhite,[40] K. Sliwa,[57] J.R. Smith,[7] F.D. Snider,[17] R. Snihur,[34] M. Soderberg,[35] A. Soha,[7] S. Somalwar,[53] V. Sorin,[36] J. Spalding,[17] F. Spinella,[47] T. Spreitzer,[34] P. Squillacioti,[47] M. Stanitzki,[61] A. Staveris-Polykalas,[47] R. St. Denis,[21] B. Stelzer,[8] O. Stelzer-Chilton,[43] D. Stentz,[39] J. Strologas,[38] D. Stuart,[10] J.S. Suh,[28] A. Sukhanov,[18] H. Sun,[57] T. Suzuki,[56] A. Taffard,[24] R. Takashima,[41] Y. Takeuchi,[56] K. Takikawa,[56] M. Tanaka,[2] R. Tanaka,[41] M. Tecchio,[35] P.K. Teng,[1] K. Terashi,[51] J. Thom[d],[17] A.S. Thompson,[21] E. Thomson,[46] P. Tipton,[61] V. Tiwari,[12] S. Tkaczyk,[17] D. Toback,[54] S. Tokar,[14] K. Tollefson,[36] T. Tomura,[56] D. Tonelli,[47] S. Torre,[19] D. Torretta,[17] S. Tourneur,[45] W. Trischuk,[34] R. Tsuchiya,[58] S. Tsuno,[41] N. Turini,[47] F. Ukegawa,[56] T. Unverhau,[21] S. Uozumi,[56] D. Usynin,[46] S. Vallecorsa,[20] N. van Remortel,[23] A. Varganov,[35] E. Vataga,[38] F. Vázquez[i],[18] G. Velev,[17] G. Veramendi,[24] V. Veszpremi,[49] R. Vidal,[17] I. Vila,[11] R. Vilar,[11] T. Vine,[31] I. Vollrath,[34] I. Volobouev[n],[29] G. Volpi,[47] F. Würthwein,[9] P. Wagner,[54] R.G. Wagner,[2] R.L. Wagner,[17] J. Wagner,[26] W. Wagner,[26] R. Wallny,[8] S.M. Wang,[1] A. Warburton,[34] S. Waschke,[21] D. Waters,[31] M. Weinberger,[54] W.C. Wester III,[17] B. Whitehouse,[57] D. Whiteson,[46] A.B. Wicklund,[2] E. Wicklund,[17] G. Williams,[34] H.H. Williams,[46] P. Wilson,[17] B.L. Winer,[40] P. Wittich[d],[17] S. Wolbers,[17] C. Wolfe,[13] T. Wright,[35] X. Wu,[20] S.M. Wynne,[30] A. Yagil,[17] K. Yamamoto,[42] J. Yamaoka,[53] T. Yamashita,[41] C. Yang,[61] U.K. Yang[j],[13] Y.C. Yang,[28] W.M. Yao,[29] G.P. Yeh,[17] J. Yoh,[17] K. Yorita,[13] T. Yoshida,[42] G.B. Yu,[50] I. Yu,[28] S.S. Yu,[17] J.C. Yun,[17] L. Zanello,[52] A. Zanetti,[55] I. Zaw,[22] X. Zhang,[24] J. Zhou,[53] and S. Zucchelli[5]

(CDF Collaboration*)

[1] *Institute of Physics, Academia Sinica, Taipei, Taiwan 11529, Republic of China*
[2] *Argonne National Laboratory, Argonne, Illinois 60439*
[3] *Institut de Fisica d'Altes Energies, Universitat Autonoma de Barcelona, E-08193, Bellaterra (Barcelona), Spain*
[4] *Baylor University, Waco, Texas 76798*
[5] *Istituto Nazionale di Fisica Nucleare, University of Bologna, I-40127 Bologna, Italy*
[6] *Brandeis University, Waltham, Massachusetts 02254*
[7] *University of California, Davis, Davis, California 95616*
[8] *University of California, Los Angeles, Los Angeles, California 90024*
[9] *University of California, San Diego, La Jolla, California 92093*
[10] *University of California, Santa Barbara, Santa Barbara, California 93106*
[11] *Instituto de Fisica de Cantabria, CSIC-University of Cantabria, 39005 Santander, Spain*
[12] *Carnegie Mellon University, Pittsburgh, PA 15213*
[13] *Enrico Fermi Institute, University of Chicago, Chicago, Illinois 60637*
[14] *Comenius University, 842 48 Bratislava, Slovakia; Institute of Experimental Physics, 040 01 Kosice, Slovakia*
[15] *Joint Institute for Nuclear Research, RU-141980 Dubna, Russia*
[16] *Duke University, Durham, North Carolina 27708*
[17] *Fermi National Accelerator Laboratory, Batavia, Illinois 60510*
[18] *University of Florida, Gainesville, Florida 32611*
[19] *Laboratori Nazionali di Frascati, Istituto Nazionale di Fisica Nucleare, I-00044 Frascati, Italy*
[20] *University of Geneva, CH-1211 Geneva 4, Switzerland*
[21] *Glasgow University, Glasgow G12 8QQ, United Kingdom*
[22] *Harvard University, Cambridge, Massachusetts 02138*
[23] *Division of High Energy Physics, Department of Physics, University of Helsinki and Helsinki Institute of Physics, FIN-00014, Helsinki, Finland*
[24] *University of Illinois, Urbana, Illinois 61801*

[25] The Johns Hopkins University, Baltimore, Maryland 21218
[26] Institut für Experimentelle Kernphysik, Universität Karlsruhe, 76128 Karlsruhe, Germany
[27] High Energy Accelerator Research Organization (KEK), Tsukuba, Ibaraki 305, Japan
[28] Center for High Energy Physics: Kyungpook National University, Taegu 702-701, Korea; Seoul National University, Seoul 151-742, Korea; and SungKyunKwan University, Suwon 440-746, Korea
[29] Ernest Orlando Lawrence Berkeley National Laboratory, Berkeley, California 94720
[30] University of Liverpool, Liverpool L69 7ZE, United Kingdom
[31] University College London, London WC1E 6BT, United Kingdom
[32] Centro de Investigaciones Energeticas Medioambientales y Tecnologicas, E-28040 Madrid, Spain
[33] Massachusetts Institute of Technology, Cambridge, Massachusetts 02139
[34] Institute of Particle Physics: McGill University, Montréal, Canada H3A 2T8; and University of Toronto, Toronto, Canada M5S 1A7
[35] University of Michigan, Ann Arbor, Michigan 48109
[36] Michigan State University, East Lansing, Michigan 48824
[37] Institution for Theoretical and Experimental Physics, ITEP, Moscow 117259, Russia
[38] University of New Mexico, Albuquerque, New Mexico 87131
[39] Northwestern University, Evanston, Illinois 60208
[40] The Ohio State University, Columbus, Ohio 43210
[41] Okayama University, Okayama 700-8530, Japan
[42] Osaka City University, Osaka 588, Japan
[43] University of Oxford, Oxford OX1 3RH, United Kingdom
[44] University of Padova, Istituto Nazionale di Fisica Nucleare, Sezione di Padova-Trento, I-35131 Padova, Italy
[45] LPNHE, Universite Pierre et Marie Curie/IN2P3-CNRS, UMR7585, Paris, F-75252 France
[46] University of Pennsylvania, Philadelphia, Pennsylvania 19104
[47] Istituto Nazionale di Fisica Nucleare Pisa, Universities of Pisa, Siena and Scuola Normale Superiore, I-56127 Pisa, Italy
[48] University of Pittsburgh, Pittsburgh, Pennsylvania 15260
[49] Purdue University, West Lafayette, Indiana 47907
[50] University of Rochester, Rochester, New York 14627
[51] The Rockefeller University, New York, New York 10021
[52] Istituto Nazionale di Fisica Nucleare, Sezione di Roma 1, University of Rome "La Sapienza," I-00185 Roma, Italy
[53] Rutgers University, Piscataway, New Jersey 08855
[54] Texas A&M University, College Station, Texas 77843
[55] Istituto Nazionale di Fisica Nucleare, University of Trieste/ Udine, Italy
[56] University of Tsukuba, Tsukuba, Ibaraki 305, Japan
[57] Tufts University, Medford, Massachusetts 02155
[58] Waseda University, Tokyo 169, Japan
[59] Wayne State University, Detroit, Michigan 48201
[60] University of Wisconsin, Madison, Wisconsin 53706
[61] Yale University, New Haven, Connecticut 06520

(Dated: February 15, 2007)

We present a measurement of $\sigma(p\bar{p} \to W) \times \mathcal{B}(W \to e\nu)$ at $\sqrt{s} = 1.96$ TeV, using electrons identified in the forward region ($1.2 < |\eta| < 2.8$) of the CDF II detector. The data correspond to an integrated luminosity of 223 pb^{-1}. We measure $\sigma \times \mathcal{B} = 2796 \pm 13(\text{stat})^{+95}_{-90}(\text{syst}) \pm 162$ (lum) pb. Combining this result with a previous CDF measurement obtained using electrons in the central region ($|\eta| \lesssim 1$), we present the first measurement of the ratio of central-electron to forward-electron W partial cross sections $R_{\text{exp}} = 0.925 \pm 0.006(\text{stat}) \pm 0.032(\text{syst})$, consistent with theoretical predictions using CTEQ and MRST parton distribution functions.

PACS numbers: 13.38.Be, 13.85.Qk, 12.38.Qk, 14.70.Fm

*With visitors from [a]University of Athens, [b]University of Bristol, [c]University Libre de Bruxelles, [d]Cornell University, [e]University of Cyprus, [f]University of Dublin, [g]University of Edinburgh, [h]University of Heidelberg, [i]Universidad Iberoamericana, [j]University of Manchester, [k]Nagasaki Institute of Applied Science, [l]University de Oviedo, [m]University of London, Queen Mary and Westfield College, [n]Texas Tech University, [o]IFIC(CSIC-Universitat de Valencia),

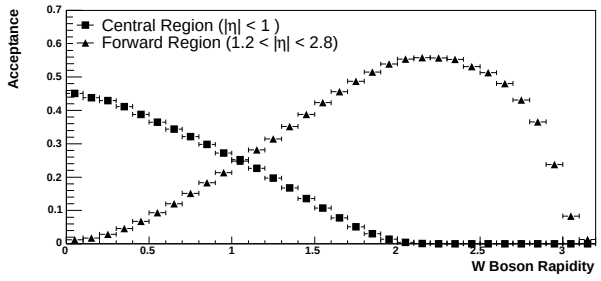

FIG. 1: Acceptance, obtained from simulation, as a function of the W boson rapidity. "Forward Region" refers to this measurement (electron pseudorapidity $1.2 < |\eta| < 2.8$) while "Central Region" refers to the analysis reported in [6] ($|\eta| <1$). The two analyses sample different regions of y_W. Areas are arbitrarily normalized.

The cross section for W boson production in $p\bar{p}$ collisions has been computed at next-to-leading order (NLO) [1] and next-to-next-to-leading order (NNLO) [2] in the strong coupling constant α_s. Experimental results can be used to test the calculation of higher order QCD contributions and the parton distribution functions (PDFs) of the proton.

The PDFs describe the momentum distributions of the elementary constituents of the colliding hadrons, and their uncertainties affect many precision measurements at both the Tevatron and the LHC [3]. A better knowledge of the PDF distributions can reduce the uncertainties on the measurements of the masses and production cross sections of the W boson and the top quark. Moreover, accurate PDF modeling of the pseudorapidity η [4] of the lepton from W boson decay is required for the use of W production as a luminosity monitor, an attractive option in the high energy regime of the LHC [5].

The momentum fractions carried by the partons in colliding hadrons determine the momentum distribution of the W boson. The W boson momentum parallel to the proton beam direction cannot be measured in $p\bar{p}$ collisions, since the longitudinal momentum of the neutrino from the W decay is not measured. However, independent measurements of the W cross section with central and forward leptons provide sensitivity to the W rapidity y_W (Fig. 1), and are a novel way to constrain the PDFs. We present the first attempt to constrain PDFs using the ratio of W boson cross sections measured with central and forward electrons. The largest experimental uncertainty, due to luminosity, cancels in this ratio. We compare our measurement to the theoretical predictions obtained with two of the most commonly used PDF sets.

The W cross section measurement presented in this Letter is obtained using data (corresponding to 223 ± 13 pb^{-1} of integrated luminosity) collected by the CDF II detector during Run II of the Fermilab Tevatron at $\sqrt{s}$ = 1.96 TeV. W bosons are identified by their decays to electrons in the forward region ($1.2 < |\eta| < 2.8$), from which we obtain the inclusive cross section times branching fraction $\sigma(p\bar{p} \to W) \times \mathcal{B}(W \to e\nu)$.

Previous Run II results on W production, based on electrons with $|\eta| \lesssim 1$ [7], were reported by both the CDF and DØ Collaborations [6, 8]. In Run I, at $\sqrt{s}$ = 1.8 TeV, DØ reported a measurement based on electrons at $|\eta| < 1.1$ and $1.5 < |\eta| < 2.5$ [9], without separating the central from the forward regions.

The CDF II detector is described in detail elsewhere [10]. An overview of the components relevant to this measurement follows. Tracking detectors inside a 1.4 T solenoidal magnetic field are used to reconstruct the charged particles' trajectories (tracks) and measure their momenta. The silicon tracking system (SVX) [11] provides precise measurement points from up to 8 radial layers of strip sensors spanning $1.3 < r < 28$ cm and covering $\pm$ 90 cm along the beam line. Surrounding the SVX is a 3.1 m long open-cell drift chamber (COT), which provides track measurements (hits) in 96 radial layers in the range $43.4 < r < 132.3$ cm [12]. The COT allows full track reconstruction in the range $|\eta| < 1$. The SVX extends the track reconstruction capability up to $|\eta| \simeq 2.8$.

Outside the tracking system, electromagnetic (EM) and hadronic (HAD) calorimeters measure the combined energy of showering particles [13]. Both central and forward EM calorimeters are instrumented with finely segmented detectors which measure the shower position at a longitudinal depth close to the typical location of the EM shower maximum. In the forward region the shower position is measured by two layers of 5 mm wide scintillating strips (PES) [14] with a stereo angle of 45 degrees. The first layer of the forward EM calorimeter is used as a preshower detector [13].

Gas Cherenkov counters measure the average number of $p\bar{p}$ inelastic collisions per bunch crossing and are used to determine the luminosity [15], with a total uncertainty of 5.8% [16].

The trigger system has three levels. The first two are based on hardware selection, while the third runs a simplified version of the offline reconstruction code on a farm of parallel processors [17, 18]. Data used in this analysis are selected by a trigger requiring missing transverse energy $\not\!\!E_T > 15$ GeV and an EM cluster in the forward calorimeter with $E_T > 20$ GeV.

The offline selection of candidate W decays begins by identifying a high-p_T electron on the basis of its EM shower. We require an energy cluster with $E_T > 20$ GeV in the fiducial region of the forward calorimeter at $1.2 < |\eta| < 2.8$. The ratio of hadronic to electromagnetic energy deposition must be small: $E_{\rm HAD}/E_{\rm EM} < 0.05$. The EM cluster is required to be isolated: the energy deposited in a cone of radius 0.4 in the $\eta - \phi$ plane around the EM cluster, excluding the EM cluster energy, must be less than 10% of the energy of the EM cluster itself. The neutrino from the W decay is identified by requiring $\not\!\!E_T > 25$ GeV.

To reduce the large (mostly multi-jet) remaining back-

ground, we compare the location and the energy deposition of the EM clusters in the calorimeter to projections of three-dimensional tracks independently reconstructed by the tracking detectors. As the full COT coverage is limited to the region $|\eta| < 1$ and its efficiency quickly falls off beyond $|\eta| = 1$, our sample is dominated by tracks seeded by the SVX [19]. Typically, tracks in the region $1.2 < |\eta| < 1.6$ have COT hit information, while those at larger $|\eta|$ do not.

The candidate events are required to have at least one track that extrapolates to the EM cluster shower centroid in the PES detector within 3 cm in the x and y coordinates. The selection is optimized by using a $Z \to ee$ data sample where one electron is detected in the central calorimeter [24] and the other one in the forward calorimeter ($Z \to ee$ control sample). The probability for matching a track to an EM cluster detected in the forward region in $Z \to ee$ events is 49.2 ± 0.5 %. To ensure full containment for the energy and momentum measurements, the z coordinate of the track extrapolated to the point of closest approach to the beam, must be within 60 cm from the nominal detector center. Finally, electron candidates must satisfy $E/p < 2$. After all requirements the sample contains 48,165 events.

The kinematic and geometric acceptance (A) for $W \to e\nu$ events is determined using the PYTHIA event generator [20] and a full simulation of the CDF II detector based on the GEANT simulation package [21]. We extract $A(y_W)$, the acceptance as a function of the W rapidity, from the simulation, and convolve it with a NNLO calculation of $d\sigma/dy_W$ [22], which depends on the PDFs. We compute the central value of the acceptance using the MRST 2001 next-to-next-to-leading-log (NNLL) PDF set [23] (in analogy with the W cross section measurement in the central region [24]) and find $A = 0.2567 \pm 0.0002$. Two different sets of next-to-leading-log (NLL) PDF sets with uncertainties (MRST01E and CTEQ6.1 [25]) are available. To estimate the uncertainty due to the choice of the PDFs we convolve $A(y_W)$ with the NLO $d\sigma/dy_W$ [24] for each PDF central value and $\pm 1\sigma$ eigenvalue. Using the CTEQ6.1 eigenvector basis set, we obtain a contribution to the acceptance uncertainty of (+1.7,-1.3)%. This value is roughly twice that obtained using the MRST01E PDF set. We use the difference between the NNLO and NLO $d\sigma/dy_W$ calculations to estimate the acceptance uncertainty due to higher-order QCD corrections ($\pm$ 0.47%).

The other uncertainties on the fraction of events passing our selection are due to the following: the modeling of detector response to hadrons and electrons, the primary vertex reconstruction, and the modeling of the p_T of the W boson. These are described below.

The vector sum of the energy of hadrons recoiling against the W boson enters the calculation of $\not\!\!E_T$. We tune the detector response to these hadrons by applying scale factors and offsets to the components of their summed energy parallel and perpendicular to the lepton momentum vector. We obtain a systematic uncertainty of $\pm$ 0.35% on the acceptance by taking a variation corresponding to three standard deviations in the tuning parameters.

The energy scale and resolution modeling of electrons are calibrated with $Z \to ee$ events and result in an uncertainty of $\pm$ 0.24%. The uncertainty on the scale as a function of E_T is determined using the E/p distribution. The simulation models the E_T-dependence well, and we include a $\pm$ 0.26% uncertainty on the acceptance due to the statistical limitations of the constraint.

We vary the amount of material that an electron passes through by $\pm 1/3$ of a radiation length, based on measurements of electron energy deposition in the preshower detector in the forward calorimeter. The resulting contribution to the acceptance uncertainty is $\pm$ 0.71%.

Differences in primary vertex reconstruction efficiency between data and simulation contribute less than 0.1% to the acceptance uncertainty. Finally, we vary the parameters of the PYTHIA model which influence the W boson p_T distribution [24] within the constraints of a CDF Run I Z boson measurement, and find the corresponding acceptance uncertainty to be less than 0.1%.

Electron identification, track matching, and E/p efficiencies are measured directly from data, using the $Z \to ee$ control sample. The track matching efficiency is corrected, using the full simulation, to account for the small kinematic differences of the Z electrons with respect to those from W decay. We also take into account the η distribution of electrons coming from W bosons. These efficiency measurements contribute the largest experimental uncertainty to the cross section measurement, and are limited by the Z statistics and the understanding of the background in the $Z \to ee$ sample. The relative uncertainties on the cross section measurement from electron identification, track matching, and E/p are 2.0%, 1.1%, and 1.0%, respectively.

The trigger efficiency is also measured from data, using independent triggers, and results in a relative uncertainty of 0.4%. The overall efficiency is reported in Table I.

Backgrounds fall into two categories: multi-jet events, where one jet mimics an isolated high-p_T electron and another jet is mismeasured in the calorimeters causing $\not\!\!E_T$; and electroweak backgrounds, $Z \to ee$ and $W \to \tau\nu$.

The multi-jet background is estimated directly from data. Multi-jet events are characterized by significant energy in the cone around the electron and small $\not\!\!E_T$ [24]. We assume that these two variables are not correlated and estimate the number of background events in the signal region using control regions defined by either low $\not\!\!E_T$ or high energy in the isolation cone. We vary the cuts on $\not\!\!E_T$ and isolation that define the control region and obtain a relative systematic uncertainty of 50% on the multi-jet background estimate of 1.8%. We check this calculation by determining the fraction of jets that pass our electron criteria and applying this fraction to multi-jet events with large $\not\!\!E_T$. We obtain good agreement.

The electroweak backgrounds are estimated using simulation. We separately calculate the fraction of $Z \to ee$

and $W \to \tau\nu$ events passing our selection. These fractions are then normalized to data using the theoretical value for the ratio of $\sigma(Z)/\sigma(W)$ [2] and assuming lepton universality for the $W \to \tau\nu$ decays. Background fractions from these processes are estimated to be 2.2% and 0.9% for $W \to \tau\nu$ and $Z \to ee$ respectively.

We show the M_T [4] distribution for both the signal events and background contributions in Fig. 2. The sum of signal simulation and background matches the data well.

The cross section measurement depends on the number of events passing the selection, the luminosity of the sample, the acceptance, efficiencies and backgrounds [24] (see Table I). We measure the inclusive cross section to

TABLE I: Number of selected events, geometric and kinematic acceptance, overall efficiency and expected number of background events.

$W \to e\nu$ candidates	48165	
Background multi-jet	846 $\pm$ 57 (stat)	$\pm$ 423 (syst)
Background $Z \to ee$	417 $\pm$ 5 (stat)	
Background $W \to \tau\nu$	1070 $\pm$ 12 (stat)	
Acceptance A	0.2567 $\pm$ 0.0002 (stat)	$^{+0.0051}_{-0.0042}$ (syst)
Efficiency $\epsilon_{\rm TOT}$	0.2863 $\pm$ 0.0042 (stat)	$^{+0.0060}_{-0.0061}$ (syst)

be $\sigma \times \mathcal{B} = 2796 \pm 13(\text{stat})^{+95}_{-90}(\text{syst}) \pm 162(\text{lum})$ pb, consistent with previous CDF results obtained with leptons detected in the central region and with theoretical predictions [24].

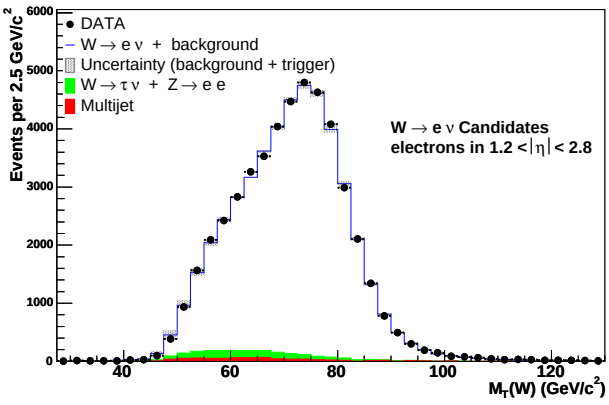

FIG. 2: M_T distribution for $W \to e\nu$ candidates (circles). The histogram is the sum of the expected background and the predicted (from simulation) signal spectrum.

The correct PDF must give the same total W cross section for central and forward electrons, within statistical and systematic uncertainties. It follows that the ratio of partial cross sections $\sigma_p = \sigma \times \mathcal{B} \times A$, where A is the kinematic and geometric acceptance, is equal to the true ratio of acceptances for the two regions. This experimental ratio can then be compared with acceptance ratios predicted by any set of PDFs. The cross section based on central electrons, using the same PDF as used above for the forward electron measurement [24], is $\sigma \times \mathcal{B}$ = 2771 $\pm$14(stat)$\pm$47(syst) pb, after removing uncertainties due to PDFs, luminosity, renormalization scale and NLO/NNLO effects. The resulting σ_p, measured for reconstructed electrons with $E_T > 25$ GeV, $|\eta| \lesssim 1$ [7] and $\not\!\!E_T > 25$ GeV is $\sigma_p^{\rm cen}$ = 664 $\pm$3(stat)$\pm$11(syst) pb. In the forward region σ_p for $E_T > 20$ GeV, $1.2 < |\eta| < 2.8$, and $\not\!\!E_T > 25$ GeV is $\sigma_p^{\rm for}$ = 718 $\pm$3(stat)$\pm$21(syst). All systematic uncertainties except those due to PDF and to NLO/NNLO effects, are assigned to σ_p. Most of the luminosity uncertainty for the overlapping data-taking period cancels in the ratio, and we assign a 1% systematic due to time-dependent luminosity uncertainty. All other uncertainties are uncorrelated. The experimental ratio is $R_{\rm exp} = \sigma_p^{\rm cen} \,/\, \sigma_p^{\rm for}$ = 0.925 $\pm$0.006(stat)$\pm$0.032 (syst). We compute also the central-to-forward ratio of acceptances $R_{\rm th}$, obtained with two different PDF sets (CTEQ6.1 and MRST01E) at NLO level. For CTEQ6.1 the ratio is $R_{\rm th} = 0.924^{+0.023}_{-0.030}(\text{PDF}) \pm 0.004$ (NLO/NNLO) and for MRST01E $R_{\rm th} = 0.941^{+0.010}_{-0.012}(\text{PDF}) \pm 0.004$ (NLO/NNLO), where "PDF" indicates the uncertainty obtained by varying the eigenvalues relative to a given PDF set. We use the prescription in [24] to compute these uncertainties.

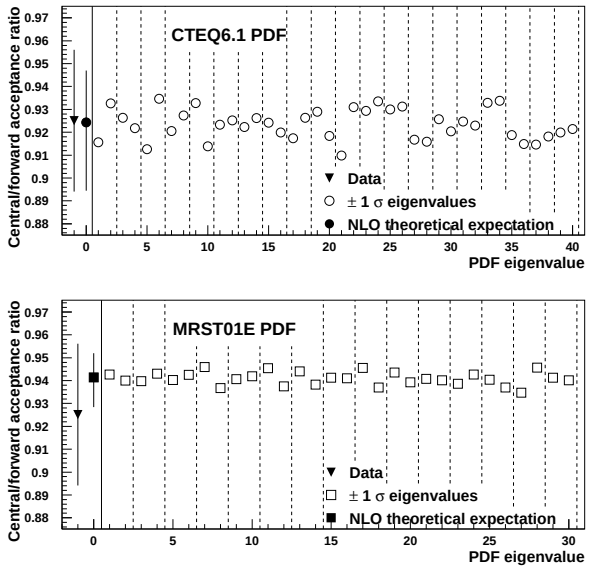

FIG. 3: The ratio of central to forward electron acceptances, as a function of the $\pm 1\sigma$ eigenvalue of CTEQ6.1 (top) and MRST01E (bottom) PDF sets. Dashed lines separate eigenvectors.

Figure 3 shows the experimental ratio of partial cross sections (solid triangles) compared to the CTEQ6.1 (upper plot) and MRST01E (lower plot) acceptance ratios (solid circle and square). The data measurement is independent of PDFs. The ratios of acceptances are also computed varying each PDF eigenvalue by $\pm 1\sigma$ (giving 40 values for CTEQ6.1 and 30 for MRST01E) and are shown as open circles and squares. Data and both PDF sets agree within uncertainties, though the central values for MRST01E and CTEQ6.1 are slightly shifted with respect to each other. The CTEQ6.1 has a larger uncertainty and some of the individual $\pm 1\sigma$ eigenvalues show a sizeable deviation from the central value. This is notably the case for eigenvector 1 (PDF eigenvalues 1 and 2 in Fig. 3), in which the dominant contribution is due to the u-valence quark distribution, and eigenvector 3 (PDF eigenvalues 5 and 6), in which the most important contribution is due to the d-valence quark distribution. These eigenvectors generally impact W boson measurements at the Tevatron, in particular the W mass measurement. Other large variations are visible for PDF eigenvalues 9 and 10 (eigenvector 5) and 19 and 20 (eigenvector 10), in which the dominant contribution is due to sea quarks and gluons. These eigenvectors are important for the W rapidity distribution at the LHC.

Recently, a calculation of $R_{\rm th}$ at NNLO became available. The calculation takes into account the spin correlation between electron and neutrino, and the experimental selection of the analysis described in this paper. Using the MRST PDF at the appropriate order in α_s, the authors find $R_{\rm th} = 0.9266 \pm 0.0019$, in good agreement with our measurement [26].

In summary, we have measured the W inclusive production cross section with electrons identified at large pseudorapidities ($1.2 < |\eta| < 2.8$) to be $\sigma \times \mathcal{B} = 2796 \pm 13(\text{stat})^{+95}_{-90}(\text{syst}) \pm 162(\text{lum})$ pb. We have measured a partial cross section using forward electrons $\sigma \times \mathcal{B} \times A = 718 \pm 3(\text{stat}) \pm 21(\text{syst})$ pb and the ratio of central-electron to forward-electron partial cross sections $R_{\rm exp} = 0.925 \pm 0.006(\text{stat}) \pm 0.032(\text{syst})$.

We thank the Fermilab staff and the technical staffs of the participating institutions for their vital contributions. This work was supported by the U.S. Department of Energy and National Science Foundation; the Italian Istituto Nazionale di Fisica Nucleare; the Ministry of Education, Culture, Sports, Science and Technology of Japan; the Natural Sciences and Engineering Research Council of Canada; the National Science Council of the Republic of China; the Swiss National Science Foundation; the A.P. Sloan Foundation; the Bundesministerium für Bildung und Forschung, Germany; the Korean Science and Engineering Foundation and the Korean Research Foundation; the Particle Physics and Astronomy Research Council and the Royal Society, UK; the Russian Foundation for Basic Research; the Comisión Interministerial de Ciencia y Tecnología, Spain; the European Community's Human Potential Programme under contract HPRN-CT-2002-00292; and the Academy of Finland.

[1] G. Altarelli, R. K. Ellis, and G. Martinelli, Nucl. Phys. **B 157**, 461 (1979); J. Kubar-Andre and F. E. Paige, Phys. Rev. D **19**, 221 (1979); K. Harada, T. Kaneko, and N. Sakai, Nucl. Phys. **B 155**, 169 (1979) [Erratum-ibid. **B 165**, 545 (1980)]; J. Abad and B. Humpert, Phys. Lett. B **80**, 286 (1979); B. Humpert and W. L. van Neerven, Phys. Lett. B **85**, 293 (1979).

[2] R. Hamberg, W. L. van Neerven, and T. Matsuura, Nucl. Phys. **B 359**, 343 (1991) [Erratum-ibid. **B 644**, 403 (2002)]; R. V. Harlander and W. B. Kilgore, Phys. Rev. Lett. **88**, 201801 (2002).

[3] S. Frixione and M. L. Mangano, J. High Energy Phys. **0405**, 056 (2004).

[4] CDF uses two coordinate systems: cartesian and cylindrical. In the cartesian system z is the beam axis, oriented in the proton direction, and x and y define the plane perpendicular to the z axis. In the cylindrical system the z axis is the same, θ is the polar angle, ϕ is the azimuthal angle, and pseudorapidity $\eta = -\ln(\tan(\theta/2))$. Transverse energy and momentum are defined as $E_T = E \sin\theta$ and $p_T = p \sin\theta$, where E is energy measured by the calorimeter and p is momentum measured by the spectrometer. Longitudinal momentum is the component parallel to the beam. Rapidity is defined as $y = \frac{1}{2} \ln \frac{(E+p_Z)}{(E-p_Z)}$. The missing E_T ($\vec{\not\!\!E}_T$) is defined by $\vec{\not\!\!E}_T = -\sum_i E_T^i \hat{n}_i$, where i is the calorimeter tower number with $|\eta| < 3.6$ and $\hat{n}_i$ is a unit vector perpendicular to the beam axis and pointing at the i^{th} calorimeter tower. We also define $\not\!\!E_T = |\vec{\not\!\!E}_T|$. The transverse mass, M_T, is defined using energy transverse to the beam direction: $M_T c^2 = \sqrt{2E_T \not\!\!E_T (1 - \cos\Delta\phi)}$, where $\Delta\phi$ is the azimuthal angle between the electron and the $\not\!\!E_T$.

[5] M. Dittmar, F. Pauss, and D. Zurcher, Phys. Rev. D **56**, 7284 (1997).

[6] D. Acosta *et al.*, (CDF Collaboration), Phys. Rev. Lett. **94**, 091803 (2005).

[7] In the CDF analysis the central electron candidate is required to be measured by the central EM calorimeter and no requirement on its η is set.

[8] The DØ Collaboration, DØ Note 4403-CONF.

[9] S. Abachi *et al.*, (DØ Collaboration), Phys. Rev. Lett. **75**, 1456 (1995).

[10] D. Acosta *et al.*, (CDF Collaboration), Phys. Rev. D **71**, 032001 (2005).

[11] A. Sill *et al.*, Nucl. Instrum. Methods A **447**, 1 (2000); A. Affolder *et al.*, Nucl. Instrum. Methods A **453**, 84 (2000).

[12] T. Affolder *et al.*, Nucl. Instrum. Methods A **526**, 249 (2004).

[13] L. Balka *et al.*, Nucl. Instrum. Methods A **267**, 272 (1988); M. Albrow *et al.*, Nucl. Instrum. Methods A **480**, 524 (2002).

[14] G. Apollinari *et al.*, Nucl. Instrum. Methods A **412**, 515 (1998).
[15] D. Acosta *et al.*, Nucl. Instrum. Methods A **461**, 540 (2001).
[16] S. Klimenko, J. Konigsberg, and T. M. Liss, Fermilab Report No. FERMILAB-FN-0741.
[17] B. L. Winer, Int. J. Mod. Phys. A **16** S01C, 1169 (2001).
[18] K. Anikeev *et al.*, Comput. Phys. Commun. **140**, 110 (2001).
[19] C. Hays *et al.*, Nucl. Instrum. Methods A **538**, 249 (2005).
[20] T. Sjöstrand *et al.*, Comput. Phys. Commun. **135**, 238 (2001). We use PYTHIA version 6.216.
[21] R. Brun and F. Carminati, CERN Program Library Long Writeup, W5013, 1993 (unpublished), version 3.15.
[22] C. Anastasiou *et al.*, Phys. Rev. D **69**, 094008 (2004).
[23] A. D. Martin *et al.*, Eur. Phys. J. C **28**, 455 (2003).
[24] A. Abulencia *et al.* (CDF Collaboration), hep-ex/0508029 (2005), submitted to Phys. Rev. D.
[25] J. Pumplin *et al.*, J. High Energy Phys. **0207**, 012 (2002).
[26] K. Melnikov and F. Petriello, Phys. Rev. D **74**, 114017 (2006).